Appl. Phys. B 89, 539–542 (2007)
DOI: 10.1007/s00340-007-2829-x

Applied Physics B
Lasers and Optics

Rapid communication

P. CAMY
J.L. DOUALAN
A. BENAYAD
M. VON EDLINGER
V. MÉNARD
R. MONCORGÉ✉

Comparative spectroscopic and laser properties of Yb^{3+}-doped CaF_2, SrF_2 and BaF_2 single crystals

Centre Interdisciplinaire de Recherches Ions et Lasers (CIRIL), UMR 6637, CEA-CNRS-ENSI Caen, Université de Caen, 6 boulevard Maréchal Juin, 14050 Caen, France

Received: 24 July 2007/Revised version: 4 October 2007
Published online: 31 October 2007 •

ABSTRACT We present the spectroscopic properties and room-temperature cw tunable laser operation of Yb^{3+}-doped CaF_2, SrF_2 and BaF_2 single crystals grown and studied in the same conditions. Emission cross sections, lifetimes, laser thresholds, laser slope efficiencies and laser wavelength tuning ranges are compared. It appears that Yb^{3+}-doped BaF_2 might be more promising for diode-pumped high power laser operation.

PACS 42.55.Rz; 42.70.Hj

1 Introduction

Yb^{3+}-doped CaF_2 has been proved in recent years to be one of the most attractive Yb^{3+} laser materials for different reasons: (i) the demonstration of broadly tunable, high-power and short-pulse laser operation with one of the best compromises in terms of averaged output power and pulse width [1–3], (ii) its ease of use, because of its cubic structure, and its good adaptation to fiber amplifier laser wavelengths, for bi-frequency laser operation and THz wave generation [4], (iii) the possibility of growing very large size and high-quality crystals [5] combined with an excellent thermal conductivity (comparable to the 11 W m^{-1} K^{-1} value found for undoped YAG) [5, 6] and a very high damage threshold (~ 53 J/cm^2, thus nearly three times larger than that of Yb:YAG, according to [7]), which gives the possibility of using Yb^{3+}:CaF_2 as laser amplifiers in high averaged power/high-energy laser systems with higher repetition rates.

As a consequence, works are now being pursued (i) to operate improved quality and larger size crystals in various laser systems, (ii) to investigate the spectroscopic nature of the Yb^{3+} lasing center in these highly doped (usually 2 to 6 at. %) crystals, the present interpretation being some hexameric cluster [8, 9] and (iii) to study the spectroscopic properties and the laser potential of the Yb^{3+} isotypes SrF_2 and BaF_2, which is the purpose of the present communication; each of these systems indeed offers slightly different properties (such as an even higher thermal conductivity in the case of BaF_2), and some very interesting results, with which we do not entirely agree, were already recently published concerning Yb^{3+}:SrF_2 [10].

2 Crystal growth and material properties

The Yb^{3+}-doped MeF_2 crystals (Me = Ca, Sr, Ba) were grown in our laboratory by using a conventional Bridgman technique with rf heating. A mixture of pure MeF_2 and YbF_3 powders is introduced in a graphite crucible within the growth chamber. A good vacuum ($< 10^{-5}$ mbar) is then realized before introducing Ar and CF_4 gases to reduce oxygen and water pollution. The crystal growth is carried out with a pulling rate of 4.5 mm/h. After the end of the growth process the crystals are cooled to room temperature within 24 h. Crystals of 2 at. % and 3 at. % were obtained in this way. The exact rare earth dopant concentration of the crystals was measured by ICP (inductively coupled plasma) analysis (see Table 1).

3 Spectroscopic measurements

Spectroscopic properties of the grown single crystals have been investigated by recording near-infrared absorption and emission spectra as well as determining fluorescence lifetimes and calculating cross sections.

3.1 *Absorption spectra*

Room-temperature absorption spectra were obtained by using a Perkin-Elmer Lambda 9 spectrophotometer. The thus calculated absorption cross section spectra are presented in Fig. 1. All the samples show the characteristic broad absorption band of the Yb^{3+} ions in such hosts with one principal maximum and a secondary one, though these maxima differ in position, width and intensity. CaF_2 is found to have peaks at 980 nm (FWHM of 22 nm) and 923 nm, in good agreement with former published values [1]. The intensity ratio between these two maxima is 2.3 with a cross section of 5.4×10^{-21} cm^2 at 980 nm. In the case of SrF_2, we observed a noticeably more intensive (9.1×10^{-21} cm^2) but narrower (FWHM of 8.3 nm) major maximum at 976.5 nm, whereas the

✉ Fax: +33-2-31-45-25-57, E-mail: richard.moncorge@ensicaen.fr

Laser host	CaF_2	SrF_2	BaF_2
Peak absorption cross section $\sigma_{a,max}$ (10^{-21} cm^2)	5.4	9.1	9.4
Wavelength at peak λ ($\sigma_{a,max}$) (nm)	979.8	976.5	975.5
FWHM (nm)	22	8.3	7.3
Int. ratio between maximum and secondary peaks	2.3	4.2	4.7
Thermal conductivity ($W\,m^{-1}\,K^{-1}$)*	9.7	8.3	11.7
Laser wavelength λ_L (nm)	1049	1046	1045
Emission cross section σ_e (λ_L) (10^{-21} cm^2)	1.6	1.5	1.4
Density of Yb^{3+} ions	6.35×10^{20} cm^{-3} 2.59%	5.87×10^{20} cm^{-3} 2.89%	3.56×10^{20} cm^{-3} 2.12%
Lifetime τ (ms)	2.4	2.9	2.6
Tunability range (nm)	60	59	54
Slope efficiency (%)	54	53	44
Laser threshold (mW)	76	95	107

* undoped materials (Crystran Ltd., www.crystran.co.uk, www.vidrine.com/iropmat4.htm)

TABLE 1 Spectroscopic and laser parameters of Yb^{3+}-doped CaF_2, SrF_2 and BaF_2

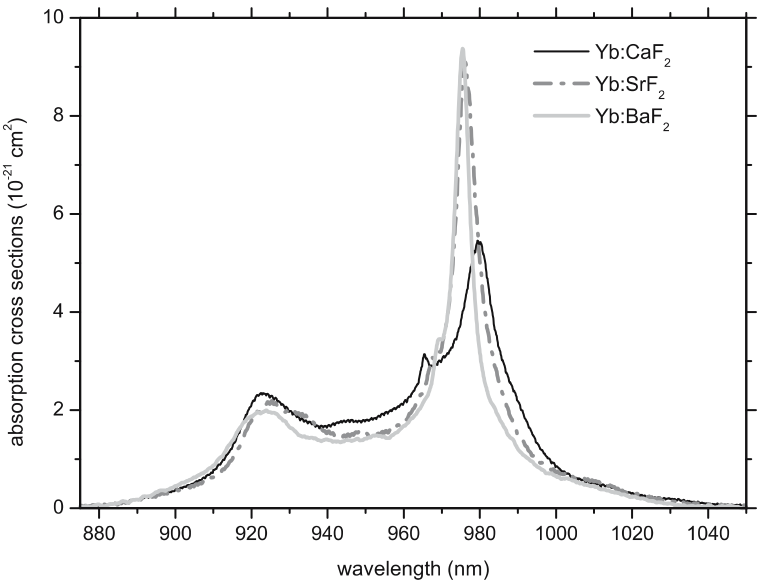

FIGURE 1 Absorption cross section spectra of Yb^{3+}-doped CaF_2, SrF_2 and BaF_2

other parts of the spectrum, including the secondary maximum at 925 nm, have intensities of the same order of magnitude as in CaF_2 leading consequently to an intensity ratio of about 4.2. BaF_2 bears more resemblance to SrF_2 than to CaF_2, showing a peak at 975.5 nm with a FWHM of 7.3 nm and a height similar to SrF_2, while we observe an intensity ratio of 4.7. The small third peak emerging at 965.5 nm and 969.5 nm respectively could be due to a marginal population of Yb^{3+} ions in O_h symmetry [8, 11]. Furthermore, it is noteworthy that the cross section of the absorption peak at 976.5 nm found here in Yb^{3+}:SrF_2 is 50% superior to the value recently reported by Siebold et al. [10], while the secondary maxima have about the same size. This may be due to different crystal composition or some different spectral resolution in the absorption measurements.

3.2 *Fluorescence lifetime*

Fluorescence decay measurements on crystals and powders were performed by using a Q-switched Nd:YAG pumped OPO (optical parametric oscillator) laser. The use of powders allowed us to eliminate lifetime lengthening reabsorption effects. At similar dopant concentration ($\sim$ 2 at. %) both SrF_2 (2.8 ms) and BaF_2 (2.6 ms) show longer lifetimes than CaF_2 (2.4 ms). Here again in the case of SrF_2, our value considerably differs from that reported in [10] (i.e. 4.8 ms).

3.3 *Emission spectra*

A lock-in amplifier, a monochromator and a photomultiplier tube were used to detect fluorescence signals. Wavelength-selective excitation around 920 nm was provided by a cw Ti:sapphire laser. Again, these measurements were performed on crystals and powders to discriminate the effects of reabsorption. The emission cross sections shown in Fig. 2 have been obtained by combining the reciprocity method for the short wavelengths and the method of Fuchtbauer–Ladenburg for the longest ones [12], thus reducing errors due to reabsorption and noise. These emission cross section spectra indicate a potential for wide tuning range and short pulse generation for all three types of fluoride crystals, but there are nevertheless differences between them. The intensities and positions of the major maxima are comparable to those obtained in absorption, which merely come from the ratio of the partition functions for the upper and lower multiplets of the Yb^{3+} ions, which was assumed to be equal to that found in the case of Yb^{3+}:CaF_2, i.e. $Z_l/Z_u = 1.12$ [13]. Compared to CaF_2, the major emission peaks of Yb^{3+}-doped SrF_2 and BaF_2 are shifted to shorter wavelengths and clearly narrower.

3.4 *Gain cross section spectra*

On the basis of the data obtained above we calculated the gain cross sections $\sigma_g = \beta\sigma_e - (1-\beta)\sigma_a$, in order to obtain a preliminary perception of the tuning ranges. Figure 3 compares these cross sections for different potential population inversion values β. Though these curves extend towards shorter wavelengths in the case of Yb^{3+}-doped SrF_2 and BaF_2, their shapes remain very similar to that found for Yb^{3+}-doped CaF_2.

4 Laser experiments

Laser action on 4-mm-thick samples of CaF_2, SrF_2 and BaF_2, prepared with parallel and uncoated end faces, has been obtained, pumping by a cw Ti:sapphire laser at 926 nm in the

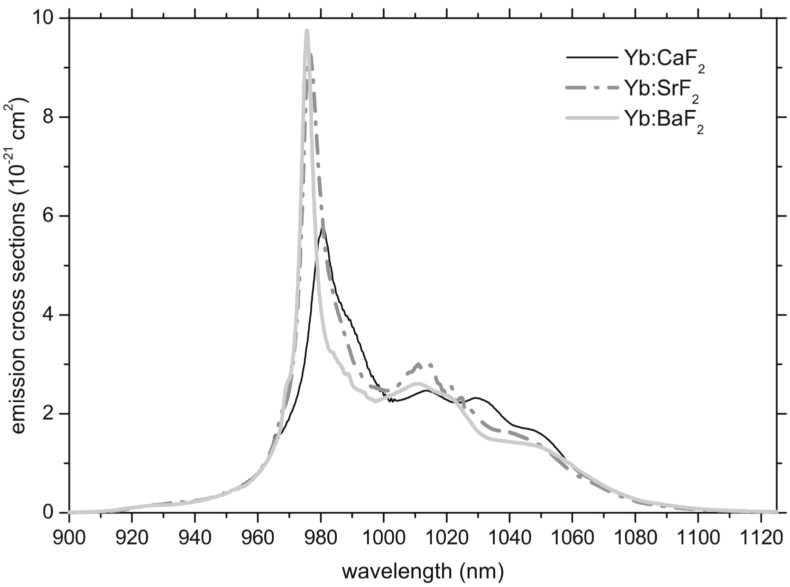

FIGURE 2 Emission cross section spectra of Yb^{3+}-doped CaF_2, SrF_2 and BaF_2

case of CaF_2 and SrF_2 and at 923 nm in the case of BaF_2. Several experimental arrangements were tried to compare the different crystals, the best results being obtained in the following conditions.

4.1 *Experimental setup*

A simple plano-concave cavity, with an output mirror of transmission $T = 5\%$ between 980 and 1100 nm and having a 10 cm radius of curvature, and a cavity length close to the stability limit, was used. The samples were mounted at the waist of the resonator, as close as possible to the input dichroic mirror, and the pump beam was focused onto the crystal by a 10 cm focal length achromatic antireflection-coated lens. For tunable laser operation a single-plate Lyot filter was inserted at the Brewster angle inside the laser cavity. All the laser results were obtained at room temperature without any cooling system.

4.2 *Laser slope efficiencies*

Figure 4 shows the laser output power versus absorbed pump power for the three crystals. Absorbed pump power was determined taking into account both the single-pass crystal absorption and the pump light reflected by the output mirror. Single-pass absorption was 47%, 38% and 27% for Yb^{3+}-doped CaF_2, SrF_2 and BaF_2, respectively, and 77% of the transmitted pump intensity was reflected back by the output mirror. It should be noted that the maximum incident pump powers of the Ti:sapphire laser (pumped by an argon laser) were slightly different for the three laser curves. Without any selective element in the cavity, laser emission occurred at 1049, 1046 and 1045 nm for CaF_2, SrF_2 and BaF_2, respectively, which means, according to the gain cross sections, a population inversion below 15% in all the cases.

4.3 *Laser wavelength tunability*

By inserting the Lyot filter mentioned above, according to their broad emission cross section spectra, similar tuning ranges, up to 60 nm, were achieved (see Fig. 5) in the case

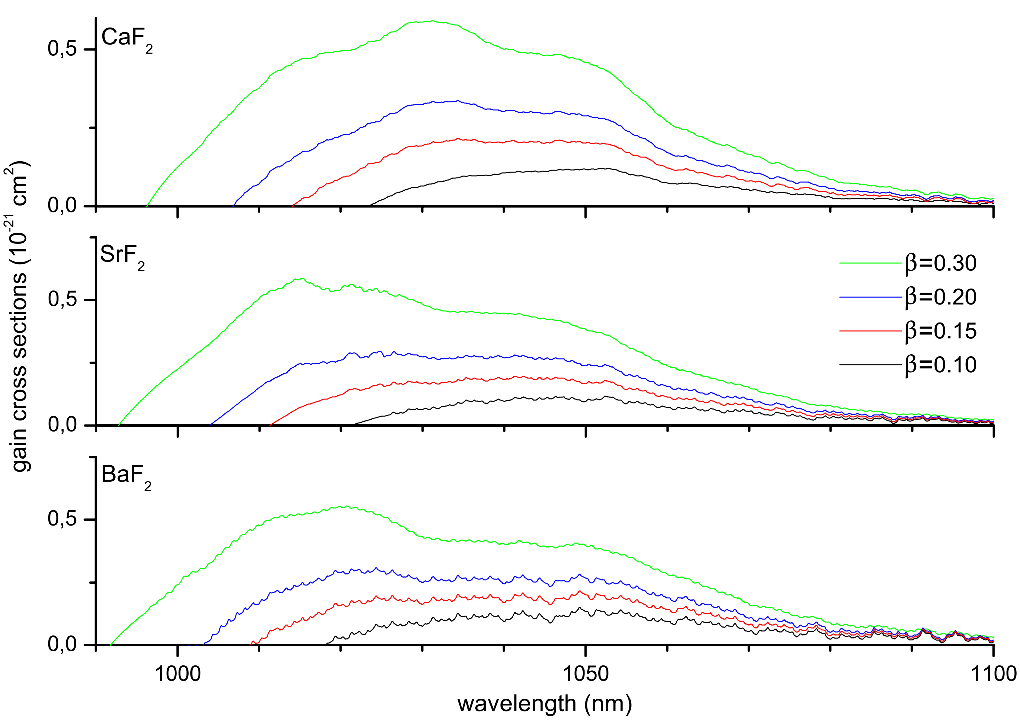

FIGURE 3 Gain cross section spectra for various population inversion values β

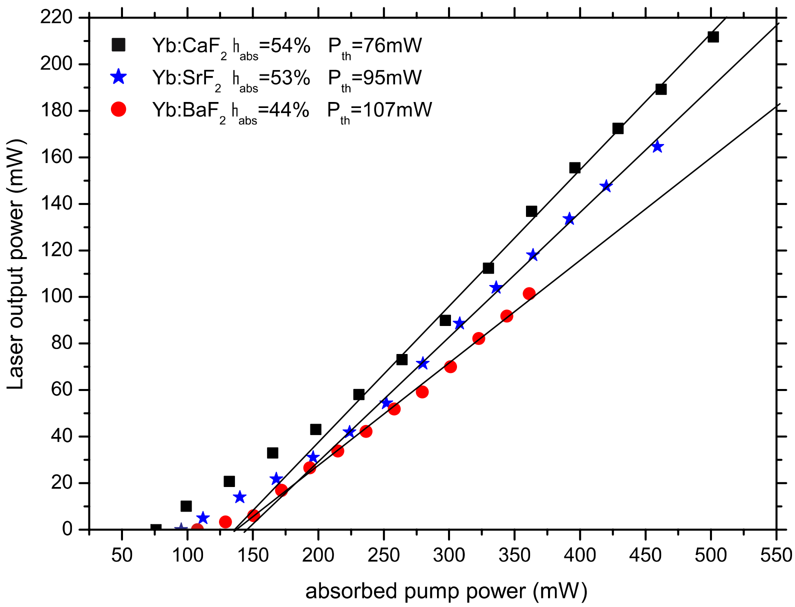

FIGURE 4 Laser output versus absorbed pump power curves

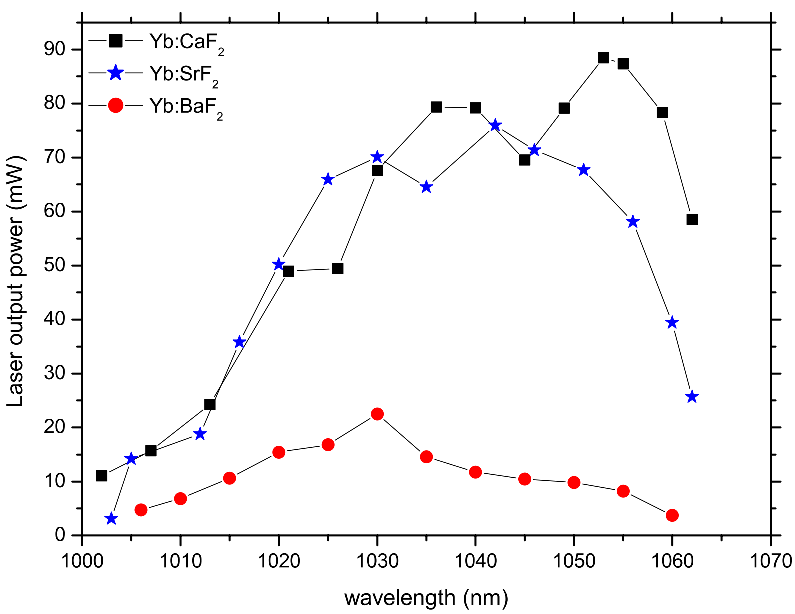

FIGURE 5 Laser wavelength tuning curves

of Yb^{3+}-doped CaF_2, SrF_2 and BaF_2. In fact, beyond 1063 nm the laser wavelength tunability was limited by the selectivity of the birefringent filter. Laser wavelength tunability should be easily extended to 1080 nm by using another selective element like a prism [10]. The reduced output power obtained in the case of Yb^{3+}:BaF_2 is likely due to a lower Yb^{3+} dopant concentration. Laser thresholds and laser efficiencies remain comparable. Table 1 recapitulates the obtained data for the three matrices.

5 Conclusion

The spectroscopic properties and room-temperature cw tunable laser operation of Yb^{3+}-doped MeF_2 (Me = Ca, Sr, Ba) single crystals grown in our laboratory have been reported and compared.

Emission cross sections, lifetimes, laser thresholds, laser slope efficiencies and laser wavelength tuning ranges are comparable. However, the absorption peaks occur at shorter wavelengths and appear both more intense and narrower in the case SrF_2 and BaF_2 than in the case of CaF_2, which is not quite well understood at the moment but is certainly interesting for pumping the samples more efficiently. In particular, though the present performance of Yb^{3+}:BaF_2 seems less interesting than the others, this system, once optimized, might be more promising, in the case of diode pumping around 975 nm, because of a peak absorption cross section and a thermal conductivity which are clearly larger than in the other systems.

Future works are now in progress to operate both Yb^{3+}-doped SrF_2 and BaF_2 materials by using more adapted crystal compositions and optimized laser conditions both in the cw and the ultra-short-pulse laser regimes.

REFERENCES

1. V. Petit, J.L. Doualan, P. Camy, V. Ménard, R. Moncorgé, Appl. Phys. B **78**, 681 (2004)
2. A. Lucca, G. Debourg, M. Jacquemet, F. Druon, F. Balembois, P. Georges, P. Camy, J.L. Doualan, R. Moncorgé, Opt. Lett. **29**, 1879 (2004)
3. A. Lucca, G. Debourg, M. Jacquemet, F. Druon, F. Balembois, P. Georges, P. Camy, J.L. Doualan, R. Moncorgé, Opt. Lett. **29**, 2767 (2004)
4. R. Czarny, M. Alouini, X. Marcadet, S. Bansropun, J.L. Doualan, R. Moncorge, J.F. Lampin, M. Krakowski, D. Dolfi, in *2006 International Topical Meeting on Microwave Photonics* (IEEE Cat. No. 06EX1314) (IEEE, Piscataway, NJ, USA), pp. 290–292
5. J.L. Doualan, P. Camy, R. Moncorgé, E. Daran, M. Couchaud, B. Ferrand, J. Fluorine Chem. **128**, 459 (2007)
6. F. Druon, S. Chesnais, P. Raybaut, F. Balembois, P. Georges, R. Gaumé, G. Aka, B. Viana, S. Mohr, D. Kopf, Opt. Lett. **27**, 197 (2002)
7. M. Siebold, A. Jochmann, M. Hornung, S. Bock, J. Hein, M.C. Kaluza, S. Podleska, R. Boedefeld, in *Advanced Solid State Photonics (ASSP) 2007*, OSA paper WB15; J. Wemans, G. Figueira, N. Lopez, L. Cardosa, M. Siebold, J. Hein, F. Diaz, Yb-based regenerative amplification, in *CLEO 2007*, Munich, OSA paper CA1-5 MON, to appear
8. V. Petit, P. Camy, J.L. Doualan, R. Moncorgé, J. Luminesc. **122–123**, 5 (2007)
9. A.E. Nikiforov, A.Y. Zakharov, M.Y. Ugryumov, S.A. Kazanski, A.I. Ryskin, G.S. Shakurov, Phys. Solid State **47**, 1431 (2005)
10. M. Siebold, J. Hein, M.C. Kaluza, R. Uecker, Opt. Lett. **32**, 1818 (2007)
11. M. Ito, C. Goutaudier, Y. Guyot, K. Lebbou, T. Fukuda, G. Boulon, J. Phys.: Condens. Matter **16**, 1501 (2004)
12. L.D. DeLoach, S.A. Payne, L.L. Chase, L.K. Smith, W.L. Kway, W.F. Krupke, IEEE J. Quantum Electron. **QE-29**, 1179 (1993)
13. V. Petit, Ph.D. thesis (Thèse de Doctorat), Université de Caen/Basse-Normandie (2006)